

Synthesis of Novel Schiff Base Silicon Compound for Employing as Corrosion Inhibitor for Carbon Steel in the 1 M HCL and 3.5% NaCl Aqueous Media

Mohamed A. Abbas, Khaled Zakaria, A. Hamdy, O. M. Abo-Elenien, and Olfat E. El-Azabawy

Abstract—The inhibiting performance of a novel Schiff base silicon compound for carbon steel corrosion in 1 M HCl and 3.5 % NaCl aqueous media was evaluated using weight loss and electrochemical techniques. The compound revealed good inhibition action in both tested media even at low concentrations and the inhibition efficiency increases with increasing concentration of the inhibitor. Polarization curves show that it acts as a mixed-type inhibitor and the adsorption process obeyed Langmuir adsorption model. SEM and XRD studies were used to confirm the presence of the protective film on the carbon steel surface and morphological changes occurred as a result of corrosion process.

Key words— A. Aqueous media; B. Carbon steel; Polarization; C. Corrosion inhibition; D. SEM; XRD

I. INTRODUCTION

THE utilization of inhibitors is one of the most practical methods for protection against corrosion of carbon steel and iron in different corrosive environments [1]–[2]. Carbon steel is widely used as engineering constructional material in many industrial applications, but it undergoes severe corrosion problems. It is generally accepted that HCl and NaCl are initiated as aqueous media in the corrosion study of carbon steel alloys and almost any aqueous environment can promote corrosion, which occurs under numerous complex conditions. Most commercial inhibitor formulations include aldehyde and amines in their structure are used to protect several metals from corrosion in different aggressive media [3]–[5]. On the other hand, most well known acid inhibitors are organic

compounds that contain N, S or O atoms [6]–[9]. It is reported that a huge number of organic compounds are known to be applicable corrosion inhibitors for steel in acidic environments [10]–[11]. Such compounds typically contain nitrogen, oxygen or sulphur in a conjugated system and function via adsorption of the molecules on the metal surface, creating a barrier against corroding attack [12]–[13].

The adsorption process, and consequently the inhibition efficiency and even the inhibition mechanism depend on the electronic and structural properties of the inhibitor, the nature of the surface, the temperature and pressure of the reaction, the flow velocity as well as composition of the aggressive environment [14]. Generally, the presence of hetero-atoms in the heterogeneous organic compounds increase its tendency to resist corrosion due to the higher basicity and electron density on the hetero-atoms such as N, O and S. Accordingly, these atoms are considered to be the active centers for the process of adsorption on the metal surface [15].

One of the most widely used families of organic compounds is Schiff bases and their chemistry is essential material in many organic chemistry textbooks [16]–[17]. Generally, they are easily prepared by the condensation reaction of primary amines with carbonyl compounds. The first reports of this kind of reaction have been published by Hugo Schiff in the 1860s [18]–[19]. Several Schiff bases have recently been investigated as corrosion inhibitors for various metals and alloys in aqueous media [20]–[22]. Due to the presence of the azomethine group ($-C=N-$) in the molecule, Schiff bases should be good corrosion inhibitors. Besides the imines group, substitution of different elements also affects the inhibition properties [23]. Reportedly, it has been known earlier that a particular Schiff's base compounds reveal better inhibition effect than its corresponding amine and carbonyl compound [24].

The aim of the present study is to investigate the carbon steel corrosion inhibition in 1M HCl and 3.5% NaCl solutions in presence of novel synthesized Schiff base compound; bis (triethoxyamine thioazomethine siloxane) furfural (TATSF), using weight loss and electrochemical measurements. The effect of temperature on the inhibition efficiency of TATSF has been studied by using weight loss data. In addition, Scanning electron microscope (SEM) and X-ray diffraction

Mohamed A. Abbas, Petroleum Applications Department, Egyptian Petroleum Research Institute, Nasr City, P.B. 11727, Cairo, Egypt
Corresponding author's phone:+2201006554479; e-mail: mohamedabbas1966@yahoo.com).

Khaled Zakaria, Analysis and Evaluation Department, Egyptian Petroleum Research Institute, Nasr City, P.B. 11727, Cairo, Egypt (e-mail:khaled209eg@yahoo.com).

A. Hamdy 3Analysis and Evaluation Department, Egyptian Petroleum Research Institute, Nasr City, P.B. 11727, Cairo, Egypt (e-mail:dramal@gmail.com)

O. M. Abo-Elenien, Petroleum Applications Department, Egyptian Petroleum Research Institute, Nasr City, P.B. 11727, Cairo, Egypt (e-mail:drossamaa13@yahoo.com).

Olfat E. El-Azabawy, Petroleum Applications Department, Egyptian Petroleum Research Institute, Nasr City, P.B. 11727, Cairo, Egypt

analysis were used to study the morphological changes and corrosion products composition.

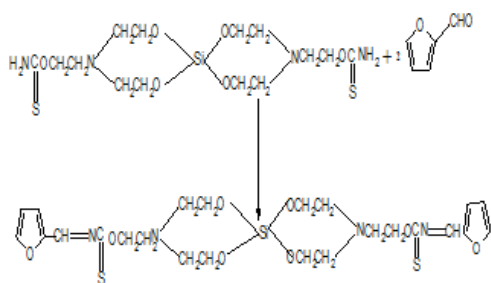
II. EXPERIMENTAL

A. Metal Sample Specification

Weight loss and electrochemical experiments were carried out on carbon steel of the following composition (wt. %): 0.19% C, 0.05% Si, 0.94% Mn, 0.009% P, 0.004% S, 0.014% Ni, 0.009% Cr, 0.034% Al, 0.016% V, 0.003% Ti, 0.022% Cu, and the rest Fe. Rectangular carbon steel coupons having dimensions of $5.6 \times 2.7 \times 0.5$ cm with an exposed total surface area of 38.54 cm^2 were used for gravimetric measurements. For electrochemical experiments, the carbon steel cylinder, embedded in epoxy resin with an exposed surface area of 1 cm^2 to the electrolyte was used as working electrode. Before doing all experiments, the surface of carbon steel was abraded with a series of emery paper (320-600-800-1000-1200) and then washed with bi-distilled water and acetone.

B. Synthesis of Schiff base Compound Inhibitor

Bis(dithioaminiethanolamine)siloxane was prepared according to our method, which is described elsewhere [25]. Then, in a three necked round bottom flask, Bis(dithioaminiethanolamine)siloxane (1mol) and furfural aldehyde (2 mol) were heated at $120 \text{ }^\circ\text{C}$ with good stirring and maintained there for 2 h. The flask was connected to a distillation system and the temperature was rapidly raised to $250 \text{ }^\circ\text{C}$ and maintained there for 2 h with constant stirring. The reaction mixture was cooled to room temperature and then separated by filtration. The chemical structure of product compound was confirmed by elemental analysis, FT-IR, and ^1H NMR spectra. The route of synthesis of the Schiff compound is shown in scheme 1.



Scheme 1. Synthesis of bis(triethoxyamine thioazomethine furfural) siloxane (TATSF).

C. Characterization Techniques

The chemical structure of product compound was confirmed by elemental analysis, FT-IR, and ^1H -NMR spectra. The elemental analyses were performed for the synthesized compound using the Vario Elementar instrument for elemental analysis. The IR Spectra were investigated using (FT-IR) Spectrometer Model Type Mattson Bench top 961. The wave number and intensities of the IR of the different types of the functional groups were determined in the range of $500\text{--}4000 \text{ cm}^{-1}$. Finally, the ^1H NMR of the prepared Schiff base silicon

compound was determined in dimethyl sulphoxide using 300MHz Spectrometer W-P-300, Bruker.

D. Solutions

The aggressive solutions of 1.0 M HCl and 3.5 % NaCl were prepared by dilution of AR grade 37% HCl and NaCl with distilled water, respectively. The concentration range of the synthesized Schiff base compound used is from 5×10^{-6} to 1×10^{-2} M/L. All solutions were prepared using bi-distilled water.

E. Gravimetric Measurements

Weight loss measurements were carried out by immersing the carbon steel coupons into aerated aggressive solutions (1 M HCl and 3.5% NaCl) in absence and presence of different concentrations of Schiff base compound at various temperatures ranging from 303 to 333 K. After the determined immersion time of 6 h, the specimens were taken out, washed, dried and weighed perfectly. The degree of surface coverage (Θ) and the inhibition efficiency ($\eta_{w\%}$) were obtained from the evaluated weight loss using the following equation:

$$\Theta = (W_o - W_{inh}) / W_o \quad (1)$$

$$\eta_{w\%} = [(W_o - W_{inh}) / W_o] \times 100 \quad (2)$$

where, W_o and W_{inh} are the weight loss values in the absence and in the presence of inhibitor, respectively. The corrosion rate, C_R ($\text{mg cm}^{-2} \text{ h}^{-1}$) was calculated using the equation [25-26];

$$CR = \frac{W}{ST} \quad (3)$$

where W is the weight loss (mg), S is the surface area of specimens (cm^2), and t is the exposure time (h).

F. Electrochemical Techniques

Carbon steel strips of the same composition embedded in araldite (a fixed material) with an exposed area of 1.0 cm^2 were used for potentiodynamic polarization and electrochemical impedance spectroscopy (EIS) studies. All the experiments were carried out at a temperature of $30 \pm 2 \text{ }^\circ\text{C}$ as per ASTM, G3-74 and G-87 [28].

Potentiodynamic polarization and impedance studies were carried out using a Radiometer Voltalab master (Model PGZ 301) with EIS software program Zsimpwin.

Three-electrode system was used, with the carbon steel sample as the working electrode, a saturated calomel electrode as the reference and a platinum wire as the counter electrode. The impedance measurements were carried out over a frequency range from 100 kHz to 50 mHz with an AC sine wave amplitude of 10 mV at the open circuit potential. For polarization measurements the potential was swapped from -800 to -300 mV with respect to OCP at a sweep rate 2 mVs^{-1} . The linear Tafel segment of anodic and cathodic curves were extrapolated to corrosion potential to obtain the corrosion current densities (I_{corr}).

G. Scanning Electron Microscope (SEM)

Scanning electron microscopy was used to get information about the changes occurred on the surface of corrosive samples before and after the addition of inhibitors. The specimens were first immersed in 1 M HCl and 3.5% NaCl solutions in the absence and presence of optimal

concentrations (0.01 M) of the tested compound for 48 h at room temperature, then taken out from the test solutions, cleaned with bi-distilled water and acetone, and dried with cool air. The SEM images were conducted using JEOL model JSM-53000 scanning electron microscope (SEM).

H. X-ray Diffraction Analysis (XRD)

To identify the corrosion products covering the metal surface and to understand the corrosive conditions that led to the corrosion of the metal, XRD analysis was used. Carbon steel coupons were immersed in the aggressive solution for 48 hrs in absence and presence of optimum concentration of the studied inhibitor. The corrosion products developed on the surface of the coupons were taken up, gently powdered and homogenized. The identification of the phases was carried out using X-ray powder diffractometer, X'PERT PRO MPD (PANalytical, Netherland). The XRD patterns were recorded with a Cu K α radiation of wavelength of 1.5406 Å operated at 40 kV/40 mA. The samples were step-scanned in the 2 θ range of 4°-80° with a step size 0.02 and a time step of 0.4s. The individual crystalline phases formed on the carbon steel surface were identified using the ICDD-PDF database.

III. RESULTS AND DISCUSSION

I. Chemical Structure Confirmation

The chemical structures of the synthesized Schiff base silicon compound were confirmed by the elemental analysis, FT-IR and ¹H NMR spectra. Elemental analysis of the compound was presented in Table 1. The data of elemental analysis confirmed the purity of the prepared inhibitors. The determined mean molecular weights have been found to be very near to that calculated theoretically. FT-IR characteristic bands and ¹H NMR characteristic peaks of the prepared inhibitors are listed in Tables 2 and 3, respectively. These data confirmed the expected functional groups and the expected hydrogen proton distribution in the prepared inhibitors, respectively.

A. Electrochemical Studies

1. EIS Measurements

EIS was used to evaluate the electrochemical corrosion properties and water uptake behavior of the coated samples [44]. The impedance data of carbon steel plotted after immersion time of 10 min in 1M HCl and 3.5% NaCl solutions in the absence and presence of different concentrations of (TATSF) ranges 10⁻⁶–10⁻² mol l⁻¹ at ambient temperatures are presented as Nyquist plots in Fig. 1. It can be seen from the figure that the diameter of the semicircle increases with the increase in inhibitor concentration in the electrolyte, indicating an increase in corrosion resistance of the material. Impedance spectra obtained at all concentration of TATSF fitted to the electrical equivalent circuits presented in Fig.2. The equivalent circuit consists of the double-layer capacitance (Q=C_{dl}) in parallel to the charge transfer resistance (R_{ct}), which was used previously to model the iron/acid interface and similar circuit have been described in the literature for the acidic corrosion inhibition of steel [30, 31]. These models reveal electrolyte resistance, R_s, coating capacitance, C_c, coating resistance, R_p,

charge transfer resistance, R_{ct}, double layer capacitance, (Q=C_{dl}) in the aqueous medium 3.5% NaCl.

TABLE I
ELEMENTAL ANALYSIS OF THE PREPARED SCHIFF BASE SILICON COMPOUND

Molecular weight	596	
Formula	C ₂₄ H ₃₂ N ₄ O ₈ S ₂ Si	
C%	Calculated	48.32
	Found	47.78
H%	Calculated	7.66
	Found	6.36
N%	Calculated	11.67
	Found	10.39
S%	Calculated	4.69
	Found	5.35
Si%	Calculated	10.73
	Found	11.17

TABLE II
FTIR BANDS OF THE SYNTHESIZED SCHIFF BASE SILICON COMPOUND

Range (cm ⁻¹)	Groups	Range (cm ⁻¹)	Groups
2924, 2880 and 1403 cm ⁻¹	—CH ₂	3348 cm ⁻¹	—CH for Furan ring
1151 cm ⁻¹	C-O-C	1639 cm ⁻¹	—C=N group
1071 cm ⁻¹	Si-alkoxy group	1471, 1403 and 1358 cm ⁻¹	—CH-C
1032 cm ⁻¹	—C=S group	1587 cm ⁻¹	—C=C Furan ring

TABLE III
1H NMR BEAKS OF THE SYNTHESIZED SCHIFF BASE SILICON COMPOUND

Range (cm ⁻¹)	Groups	Range (cm ⁻¹)	Groups
δ≈ 2.2	—CH ₂	δ≈3.4 and 3.8 triplet	—CH ₂ shielded due to attachment to —Si—O group
at δ≈ 1.7	—CH ₂	δ≈ 5.8 triplet	—CH shielded due to attachment to Furan ring
δ≈ 4.3	—NCH ₂	δ≈ 6.8& 7.1	Furan —CH groups

The existence of a single semicircle shows the occurrence of a single charge transfer process during dissolution that is unaffected by the presence of inhibitor species [30]. The depressed nature of the semicircles is a characteristic of solid electrodes; such frequency dispersion has been attributed to micro roughness and other inhomogeneities of the solid electrode [26]. The R_{ct} value is a measure of electron transfer across the surface and is inversely proportional to the corrosion rate. It is seen from Fig. 1 and Tables 4 and 5 that the presence of TATSF with all chloride solutions raises the values of R_s, R_p and R_{ct} and lowers the values of Q1 and Q2 and this effect is seen to be increased with the increase with inhibitor concentration. The constant phase elements (CPEs, Q1) with their (n) values close to 1.0 represent double layer capacitors with some pores; the CPEs decrease upon addition of TATSF and upon increase in its concentration, which are expected to cover the charged surfaces reducing the capacitive effects. It has been reported that the semicircles at high frequencies are generally associated with the relaxation of electrical double layer capacitors and the diameters of the high frequency capacitive loops can be considered as the charge transfer resistance. The impedance of the double layer capacitance element is presented by constant phase element (CPE) instead of pure capacitance as follows:

$$Z_{CPE} = (Qdl(j\omega)^{n-1}) \quad (4)$$

The exponent n has values between -1 and 1 . Inhibition efficiencies, $EF_{R_{ct}}$ (%), from impedance data were calculated through the following expression:

$$EF_{R_{ct}} = R_{ct} - \frac{R'_{ct}}{R_{ct}} \times 100 \quad (5)$$

where R_{ct} and R'_{ct} represent the charge transfer resistance in presence and absence of inhibitor, respectively.

The general shape of the curves for both media can be observed to be very similar for all the samples and this is maintained throughout the whole test period, indicating that almost no change in the corrosion mechanism occurred due to the corrosion resistant addition [31]. The parameters obtained by fitting the equivalent circuit and the calculated inhibition efficiency are listed in Tables 4 and 5.

2. Potentiodynamic polarization measurements

The potentiodynamic polarization curves of the carbon steel electrode in 1 M HCl and 3.5% NaCl solutions without and with different concentrations of (TATSF) are shown in Fig. 3. It is clearly shown that all the anodic polarization curves are parallel, which suggests the inhibitor don't affect the anodic reaction mechanism. Also, it is evident shown by Fig. 3 that the anodic curves shift towards negative potential region at all inhibitor concentration, however, generally when the change of corrosion potential is over 85 mV, the corrosion inhibitor is thought to be a cathodic or anodic type inhibitor. Therefore, TATSF behaves as mixed-type corrosion inhibitor in both tested media because the displacement in the potential is less than 85 mV [32].

Electrochemical parameters such as corrosion current density (i_{corr}), corrosion potential (E_{corr}), Tafel constants β_a and β_c , and inhibition efficiency (IE) are calculated from the Tafel plots and given in Tables 6 and 7. The inhibition efficiency was calculated from Eq. [33]:

TABLE IV

EIS PARAMETERS FOR THE CARBON STEEL IN 1 M HCL AQUEOUS MEDIUM							
Compound							
Conc.	R_s	$Q \times 10^{-7}$ $\mu F.cm^{-1}$	n	R_{ct}	Cdl $\mu F.cm^{-1}$	θ	$EF_{R_{ct}}$
1MHCl	4.7	122	0.90	91	73		
$5 \times 10^{-6} M$		91	0.80	548	43	0.84	84
$1 \times 10^{-4} M$	6.5	83	0.80	627	39.6	0.85	85
$1 \times 10^{-3} M$	7.1	76	0.77	1137	36.6	0.92	92
$5 \times 10^{-3} M$	3.2	64	0.78	1739	34.5	0.95	95
$1 \times 10^{-2} M$	0.4	53	0.80	3172	32	0.97	97

TABLE V

EIS PARAMETER FOR THE CARBON STEEL IN 3.5% NaCl AQUEUES MEDIUM						
Conc., M/L	3.5%NaCl	$5 \times 10^{-6} M$	$1 \times 10^{-4} M$	$1 \times 10^{-3} M$	$5 \times 10^{-3} M$	$1 \times 10^{-2} M$
R_s	10.59	7.758	7.96	7.96	7.395	3.91
Q	0.0002	0.000185	0.00017	0.000051	0.000058	0.000032
N	0.64	0.72	0.66	0.75	0.69	0.71
R_{po}	248	66	95	142	183	217
C_c	0.04	0.033	0.02	0.007	0.0057	0.0042
Q	0.002273	0.001472	0.001342	0.000973	0.000823	0.000741
N	0.64	0.59	0.61	0.64	0.65	0.70
R_{ct}	480	810	1008	1771	2232	2693
Cdl	2.4	1.7	1.6	1.3	1.14	0.99
θ		0.407	0.524	0.728	0.785	0.822
$EF_{R_{ct}}$		40.7	52.4	72.8	78.5	82.2

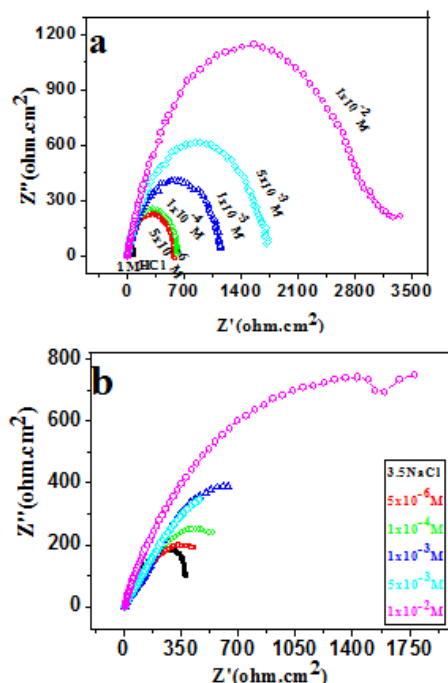


Fig. 1. Nyquist plots of TATSF for carbon steel in (a) 1M HCl and (b) 3.5% NaCl solutions

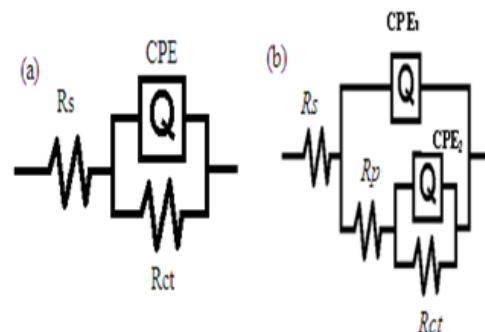


Fig. 2. The chemical equivalent circuits fitted the impedance data. (a) 1 M HCl and (b) 3.5% NaCl.

$$EF_{i_{corr}} = i'_{corr} - i_{corr} / i'_{corr} \times 100 \quad (6)$$

$$EF_{CR} = CR' - CR / CR' \times 100 \quad (7)$$

where, i_{corr} , i'_{corr} , CR and CR' are the corrosion current densities and corrosion rate with and without inhibitor. It can be seen from the data reported in Tables 6 and 7 that for TATSF in HCl media by increasing inhibitor concentration, the corrosion rate decreased and then increased at critical concentration. Moreover, the TATSF causes little change in the anodic and cathodic Tafel slopes, indicating that the inhibitors firstly adsorb onto the surface and impede the reaction by merely blocking the reaction sites of carbon steel surface without affecting the anodic and cathodic reaction mechanism [34]. On the other hand, the values of cathodic Tafel slope (β_c) and anodic Tafel slope (β_a) of the TATSF in the 3.5% NaCl changed markedly which indicates that the inhibitor affects both the anodic and cathodic reactions. However, compared with the blank solution the cathodic Tafel

slope (β_c) has noticed change, so TATSF in 3.5% NaCl media behaves as cathode-based mixed corrosion inhibitor. The cathodic reaction is the depolarization process of oxygen and the corrosion of carbon steel is controlled by the cathodic reaction; TATSF compounds form a film on the surface which reduces the diffusion rate of oxygen and suppresses the cathodic reaction thus showing good inhibition effect. However, It is clear from the data listed in Tables 6 and 7 that ,for both tested media the current densities decrease sharply with the presence of the inhibitor, which suggests that compounds adsorb on the surface therefore suppressing the cathodic reaction (oxygen reduction) and anodic reaction (metal dissolution). The inhibition efficiency of TATSF reached the maximum value of 98% and 97.9 at 10^{-2} M/L in 0.1M HCl and 3.5% NaCl respectively.

TABLE VI

POLARIZATION PARAMETERS FOR CARBON STEEL IN 1M HCL

Conc.	1MHC	5×10^{-6}	1×10^{-4}	1×10^{-3}	5×10^{-3}	1×10^{-2}
parameters						
E_{corr} mV	-524	-518	-519	-545	-522	-530
I_{corr} mA/cm	0.389	0.037	0.033	0.018	0.010	0.007
R_p ohm.cm ²	92.36	771	1180	1350	1990	4170
β_a mV	126.7	106.6	113.3	154.4	118.4	147.1
β_c mV	-146.9	-134.6	-138.	-142.3	-141.2	-140.9
CR μ m/Y	4.55	0.434	0.385	0.215	0.117	0.891
θ		0.905	0.915	0.954	0.974	0.982
EF I_{corr} %		90.5	91.5	95.4	97.4	98.2
EF CR %		90.46	91.6	95.3	97.4	98.0

TABLE VII

POLARIZATION PARAMETERS FOR CARBON STEEL IN 3.5% NaCL

Conc.	3.5%NaCl	5×10^{-6}	1×10^{-4}	1×10^{-3}	5×10^{-3}	1×10^{-2}
parameters						
E_{corr} mV	-699	-713	-680	-737	-733	-739
I_{corr} mA/cm ²	0.03	0.017	0.0127	0.006	0.0028	0.0007
R_p ohm.cm ²	1360	1600	1600	2330	2370	2700
β_a mV	109	100	95	80	77	69
β_c mV	-207	-155	-172	-123	-90	-50
CR μ m/Y	346	201	147	71.1	32.4	7.1
θ		0.433	57.7	0.80	0.907	0.977
EF I_{corr} %		43.3	57.7	80	90.7	97.7
EF CR %		41.9	57.5	79.5	90.6	97.9

A. Weight loss measurements

Inhibitor concentration effect

The corrosion rate values of carbon steel (C_R , mg cm⁻² h⁻¹) with the addition of Schiff base compound in 1 M HCl and 3.5% NaCl at different temperatures are presented in Table 8 and illustrated in Figure 4. It is obvious from the data reported in Table 8 that the weight loss decreases as the concentrations of the inhibitor was increased and the corrosion rate values decrease, consequently the inhibition efficiency increase. The corrosion inhibition of carbon steel can be attributed to the adsorption of the inhibitor at the carbon steel/aggressive solution interface. This result is due to fact that the inhibitor under study has a furan ring, nitrogen and oxygen atoms, in addition to unsaturated azomethine groups [35]. All these criteria gives the compound high adsorption ability on the carbon steel surface, hence the inhibition efficiency, increased by decreasing the interaction between the metal surface and

the corrosive ions (Cl⁻) that extensively decreases the corrosion reaction. Comparing the results of inhibition efficiency at all inhibitor concentrations in both studied media with weight loss after 6h in Table 1 revealed that the Schiff base compound has higher inhibition efficiency in 1 M HCl than in 3.5% NaCl.

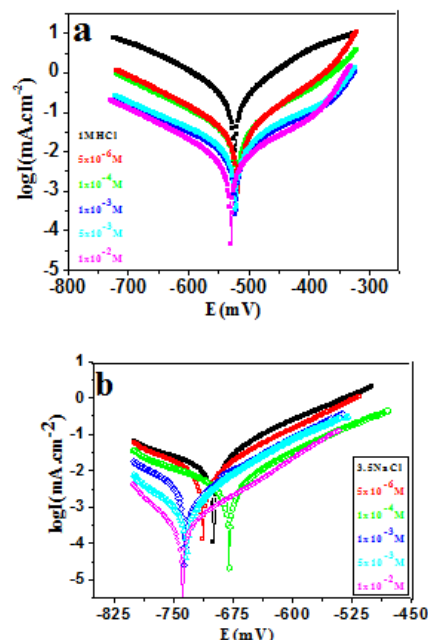


Fig.3. Polarization curves for carbon steel in (a) 1M HCl (b) 3.5% NaCl solutions in the presence of TATSF compound.

TABLE VIII

CORROSION PARAMETERS OBTAINED FROM GRAVIMETRIC MEASUREMENTS OF CARBON STEEL AFTER 6 H IMMERSIONS IN 1 M HCL AND 3.5% NaCL SOLUTIONS WITH AND WITHOUT ADDITION OF DIFFERENT CONCENTRATIONS OF SCHIFF BASE COMPOUND

T, K	Con., 10 ³	1 M HCl			3.5% NaCl		
		ΔW , (mg)	CR, (mg cm ⁻² h ⁻¹)	η_w	ΔW , (mg)	CR, (mg cm ⁻² h ⁻¹)	η_w
303	Blank	93	0.40218	--	8.455	0.03656	--
	0.5	11.1	0.04786	0.881	88.1	4.912	0.02007
	10	9.07	0.04062	0.899	89.9	3.653	0.01575
	100	6.42	0.02775	0.931	93.1	2.038	0.00881
	500	4.46	0.01931	0.952	95.2	0.989	0.00428
	1000	3.98	0.01287	0.968	96.8	0.752	0.00325
313	blank	121	0.52327	--	40.6	0.17558	--
	0.5	17.9	0.07744	0.852	85.2	25.54	0.11044
	10	14.9	0.06436	0.877	87.7	19.57	0.08463
	100	11.7	0.05076	0.903	90.3	11.90	0.05144
	500	8.1	0.03611	0.933	93.3	7.267	0.03143
	1000	5.4	0.02355	0.955	95.5	6.008	0.02599
323	blank	154	0.66598	--	75.2	0.32520	--
	0.5	28.5	0.12321	0.815	81.5	51.21	0.22146
	10	26.3	0.11388	0.829	82.9	39.93	0.17268
	100	23.1	0.09990	0.850	85.0	25.72	0.11122
	500	18.1	0.07792	0.883	88.3	15.12	0.06537
	1000	10.2	0.04462	0.934	93.4	14.74	0.06472
333	blank	162	0.70057	--	99.5	0.43029	--
	0.5	35.8	0.15483	0.779	77.9	71.24	0.30809
	10	32.7	0.14152	0.798	79.8	58.61	0.25344
	100	29.3	0.12681	0.819	81.9	38.51	0.16652
	500	24.8	0.10719	0.847	84.7	27.66	0.11962
	1000	21.2	0.09248	0.869	86.9	24.97	0.10800

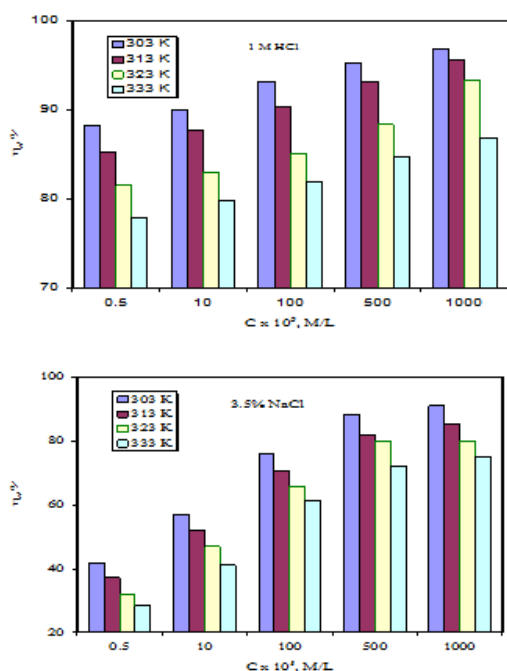


Fig. 4. The dependence of the inhibition efficiency on the concentration of Schiff base compound in both tested media at different temperatures.

Adsorption isotherms and thermodynamic parameters

It is generally accepted that the interactions of the inhibitor molecules with the active sites on the metal surface are mainly described by the adsorption isotherms [36]. Several adsorption isotherms including, Frumkin, Temkin, Freundlich, Floy-Huggins and Langmuir isotherm were attempted to fit (θ) values [37-41]. Weight loss measurements were used to evaluate the degree of surface coverage as a function of the concentration of the inhibitor (C) that was tested graphically by fitting it to various isotherms to find the best fit which describes this study. Langmuir adsorption isotherm was found to give the best description of Schiff base adsorption on carbon steel. This isotherm can be represented as [42]:

$$C_{\text{inh}}/\theta = 1/K_{\text{ads}} + C_{\text{inh}} \quad (8)$$

where, K_{ads} is the adsorptive equilibrium constant representing the interaction of the additive with the metal surface referring to the adsorption-desorption process, θ is the degree of surface coverage and C_{inh} is molar concentration of inhibitor in the bulk solution. The linear relationships of C_{inh}/θ versus C , depicted in Fig. 5 suggest that the adsorption of Schiff base compound on the carbon steel in both the media obeys Langmuir adsorption isotherm. This model assumes that the solid surface contains a fixed number of adsorption sites and each site holds one adsorbed species [43].

The constant K_{ads} is related to the standard free energy of adsorption $\Delta G_{\text{ads}}^{\circ}$ (kJ mol^{-1}) by the equation:

$$K_{\text{ads}} = 1/55.5 \exp(-\Delta G_{\text{ads}}^{\circ}/RT) \quad (9)$$

where, R is universal gas constant; $8.3144 \text{ J K}^{-1} \text{ mol}^{-1}$, T is the temperature in K . The value of 55.5 is the concentration of water in solution expressed in moles per liter. The high values of K_{ads} and negative values of $\Delta G_{\text{ads}}^{\circ}$ (Table 9) suggest that inhibitor molecules are spontaneously and strongly adsorbed

onto carbon steel surface. It is well recognized that, $\Delta G_{\text{ads}}^{\circ}$ values of -20 kJ mol^{-1} or higher are agreed with an electrostatic interaction between charged molecules and charged metal surface, physisorption but the values of -40 kJ mol^{-1} or lower associated with charge or transfer from the inhibitor molecules to the metal surface to form a coordinate covalent bond, chemisorption [44,45]. In the present work, the calculated values of $\Delta G_{\text{ads}}^{\circ}$ obtained for the inhibitor at different studied temperatures are between $-33.14 \text{ kJ mol}^{-1}$ and $-39.09 \text{ kJ mol}^{-1}$ in both studied media. These values indicate that the adsorption process of the evaluated inhibitor on the carbon steel surface may involve complex interactions (both physical and chemical adsorption). Also, it can be concluded from the Table 9 that chemical adsorption (chemisorption) is more probable for the inhibitor under investigation in 1 M HCl solution and this conclusion may also be confirmed by comparing the inhibition efficiency of the compound at different temperatures.

Adsorption thermodynamic parameters are important in studying adsorption of organic inhibitors on metal surface. The adsorption heat could be calculated according to the Van't Hoff equation [46]:

$$\ln K = -\Delta H_{\text{ads}}^{\circ}/RT + \text{constant} \quad (10)$$

To obtain the heat of adsorption, the linear regression between $\ln K_{\text{ads}}$ and $1/T$ was plotted; the relationship between $\ln K_{\text{ads}}$ and $1/T$ was shown in Figs. 5 and 6. The slope of the straight lines is equal to $(-\Delta H_{\text{ads}}^{\circ}/R)$. The adsorption heat could be approximately regarded as the standard adsorption heat ($\Delta H_{\text{ads}}^{\circ}$) under the experimental conditions [47].

Finally, the standard adsorption enthalpy $\Delta H_{\text{ads}}^{\circ}$ (kJ mol^{-1}) can be calculated by the thermodynamic basic equation [48]:

$$\Delta G_{\text{ads}}^{\circ} = \Delta H_{\text{ads}}^{\circ} - T\Delta S_{\text{ads}}^{\circ} \quad (11)$$

The value of $\Delta H_{\text{ads}}^{\circ}$ provides further information about the mechanism of corrosion inhibition. The negative value of $\Delta H_{\text{ads}}^{\circ}$ indicates that adsorption process is exothermic. An exothermic adsorption process may be chemisorption or physisorption or mixture of both, whereas endothermic process is attributed to chemisorption [49]. In exothermic adsorption process, physisorption can be distinguished from the chemisorptions on the basis of values of $\Delta H_{\text{ads}}^{\circ}$. For physisorption process the magnitude of $\Delta H_{\text{ads}}^{\circ}$ is around -40 kJ mol^{-1} or less negative while its value equals -100 kJ mol^{-1} or more negative for chemisorption [50]. All the obtained thermodynamic parameters are listed in Table 9. Clearly, it has been found that the values of $\Delta H_{\text{ads}}^{\circ}$, suggesting that the adsorption of inhibitor is an exothermic process which indicating that $\eta\%$ decreased with rise in temperature. This observation can be interpreted on the basis that at higher temperature more desorption of the adsorbed inhibitor molecules occurred from the carbon steel surface. Table 9 also showed that the values of $\Delta S_{\text{ads}}^{\circ}$ are negative being $-17.3 \text{ kJ mol}^{-1}$ in 1 M HCl and -8.0 in $3.5\% \text{ NaCl}$. These results are expected, as adsorption is an exothermic process and is always accompanied by a decrease of entropy which suggested that in the rate determining step there is association rather than dissociation [51].

TABLE IX.

THERMODYNAMIC PARAMETERS FOR THE ADSORPTION OF SCHIFF BASE COMPOUND IN 1 M HCl AND 3.5% NaCl ON CARBON STEEL SURFACE

Medium	T(K)	Slope	R ²	K _{ads} (M ⁻¹)	ΔG ⁰ _{ads} (kJmol ⁻¹)	ΔH ⁰ _{ads} (kJmol ⁻¹)	ΔS ⁰ _{ads} (Jmol ⁻¹)
1 M HCl	303	1.0336	0.9999	39211	-36.76	-17.3	62.5
	313	1.0481	0.9998	26504	-36.96		
	323	1.0754	0.9992	13680	-36.36		
	333	1.1530	0.9998	24141	-39.06		
3.5% NaCl	303	1.0927	0.9996	9302	-33.14	-8.0	83.1
	313	1.1688	0.9995	8179	-33.90		
	323	1.2371	0.9996	9051	-35.25		
	333	1.3287	0.9995	6558	-35.45		

Effect of temperature and activation parameters

It is well recognized that many changes occur on the metal surface such as rapid etching and inhibitor, desorption and decomposition and /or rearrangement [52], as a result the effect of temperature on the inhibited aggressive-metal reaction is highly complex. The impact of temperature on percentage inhibition efficiency was studied by carrying out weight loss measurements at 303-333 K containing different concentrations of Schiff base compound in 1 M HCl and 3.5% NaCl aqueous media during 6 h of immersion.

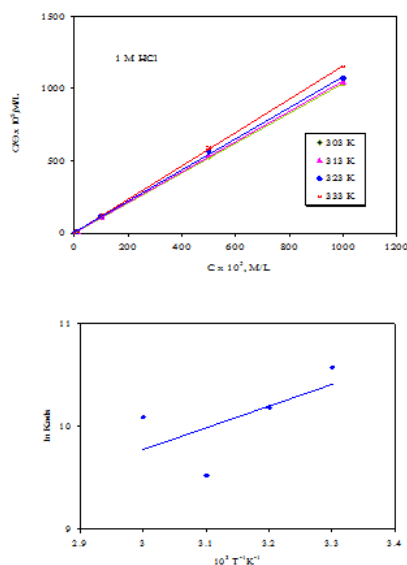


Fig.5. Adsorption isotherms for carbon steel in 1 M HCl solution at different temperatures; Langmuir adsorption isotherm and Van't Hoff plot for the carbon steel/Schiff base compound/HCl solution

The results in Table 8 indicate that the corrosion rate (C_R) increases with increasing temperature in both uninhibited and inhibited solutions. Hence, the percentage inhibition efficiency, decrease with temperature and this is may be probably due to increased rate of desorption of Schiff base compound from the carbon steel surface at higher temperatures [53]. Indeed, there is a fact that higher temperature accelerates hot-movement of the organic molecules and weakens the adsorption capacity of inhibitor on the metal surface [54].

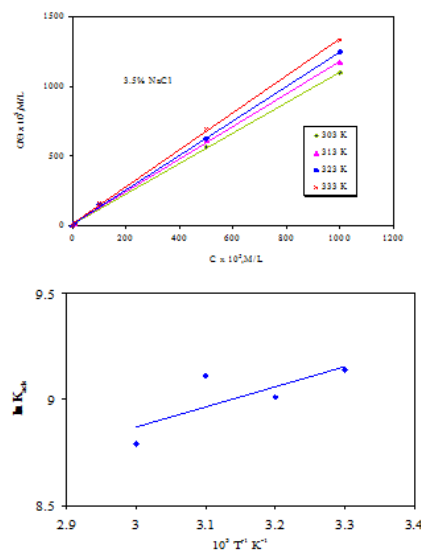


Fig.6. Adsorption isotherms for carbon steel in 3.5% NaCl solution at different temperatures; Langmuir adsorption isotherm and Van't Hoff plot for the carbon steel/Schiff base compound/NaCl solution

The relationship between the corrosion rate (C_R) of carbon steel in both tested media and temperature is often expressed by the Arrhenius equation [55];

$$C_R = A \exp(-E_a/RT) \quad (12)$$

Where, C_R is the corrosion rate, E_a is the apparent activation energy, R is the molar gas constant (8.314) JK⁻¹mol⁻¹, T is the absolute temperature, and A is the frequency factor. Figure 7 shows the plot of ln C_R against 1/T for carbon steel corrosion in 1 M HCl and 3.5% NaCl in the absence and presence of different concentrations of Schiff base compound, respectively. The apparent activation energy and pre-exponential factors can be determined by the resulting linear regression between ln C_R and 1/T, the data were presented in Table 10. The slope of each straight line gives its apparent activation energy. It can be seen from Table 10 that the apparent activation energy increased on addition of Schiff base compound in comparison to the blank solution which can be interpreted as physical (electrostatic) adsorption [56]. According to Szauer and Brandt, the increase in activation energy can be attributed to an appreciable decrease in the adsorption of the inhibitor on carbon steel surface with increase in temperature and a corresponding increase in corrosion rates occurs due to the fact that greater area of metal is exposed to the aggressive environment.

To further gain insights on the change of enthalpy and entropy of activation for the formation of the activation complex in the transition state, an alternative form of Arrhenius equation was used that is called transition state equation [57]:

$$C_R = RT/h \exp(\Delta S_a^0/R) \exp(-\Delta H_a^0/RT) \quad (13)$$

Where, C_R is the corrosion rate, h is the Planck's constant (6.626176 × 10⁻³⁴ Js), N is the Avogadro's number (6.02252 × 10²³ mol⁻¹), R is universal gas constant and T is the absolute temperature. The plot of ln C_R/T versus 1/T for carbon steel corrosion in both tested media in the absence and presence of

different concentrations of Schiff base compound is given in Fig. 8. Straight lines were obtained with slope of $(-\Delta H_a^0/R)$ and an intercept of $[(\ln(R/N_h) + (\Delta S_a^0/R))]$, from which the values of ΔH_a^0 and ΔS_a^0 respectively were computed and listed also in Table 10. Inspection of Table 10, the data revealed that the activation parameters ΔH_a^0 and ΔS_a^0 of dissolution reaction of carbon steel in both tested media in the presence of the Schiff base compound are higher than in the presence of inhibitor. The positive sign of enthalpy refers to the endothermic nature of steel dissolution process meaning that dissolution of steel is difficult [58]. In contrast, the values of entropy of activation (ΔS_a^0) listed in Table 10; show entropy of activation increased in presence of the tested inhibitor compared to free aggressive solution in both tested media. Such variation is associated with the phenomenon of ordering and disordering of inhibitor molecules on carbon steel surface. The increasing entropy of activation in the presence of inhibitor indicated that disordering is increased on going from reactant to activated complex. In other words, the adsorption process is accompanied by an increase in entropy, which is the driving force for the adsorption of inhibitor onto the carbon steel surface [59].

TABLE X
ACTIVATION PARAMETERS OF DISSOLUTION REACTION OF CARBON STEEL IN 1 M HCl AND 3.5% NaCl WITH SCHIFF BASE COMPOUND AT DIFFERENT CONCENTRATIONS

Con., 10 ⁵	1 M HCl			3.5% NaCl		
	E _a , (kJmol ⁻¹)	ΔH _a , (kJmol ⁻¹)	ΔS _a , (Jmol ⁻¹)	E _a , (kJmol ⁻¹)	ΔH _a , (kJmol ⁻¹)	ΔS _a , (Jmol ⁻¹)
blank	15.85	13.23	-208.59	66.62	64.00	-58.39
0.5	33.14	30.52	-169.15	73.90	71.29	-39.18
10	35.88	33.26	-161.61	75.23	72.62	-37.00
100	43.52	40.91	-139.30	79.71	77.10	-26.87
500	49.15	46.54	-123.91	89.17	86.55	-1.422
1000	54.50	51.88	-110.25	94.94	92.33	15.57

SEM

The formation of a protective surface film of inhibitor on the electrode surface was further confirmed by SEM observations of the electrode surface. Fig.9 shows an array of SEM images recorded for CS samples exposed for 48 h in different tested media. The morphology of specimen surface immersed in 1.0 M HCl solution is shown in Fig. 9a the micrograph reveals that in the absence of inhibitor, the surface is corroded with areas of localized corrosion. However, in presence of the inhibitor (Fig.9b), the rate of corrosion is suppressed, as can be seen from the decrease of the areas of localized corrosion and almost intact layer covered most part of the alloy surface. No signs of pitted surface were observed in this material which may be attributed to the formation of uniform film on the surface that probably develops a protective layer. The analysis via SEM has allowed us to check the degree of corrosion suffered by the various test-coupons exposed to different environments, thus it can be noticed that, the micrograph of the carbon steel electrode immersed in NaCl solution shows somewhat uniform corrosion where it consisted in corrosion spots scattered over the metallic surface as shown

in Fig. 9c. However, for the specimen immersed in NaCl solution in presence of inhibitor (Fig. 9d) the electrode surface is almost free from corrosion due to the formation of an adsorbed film of the inhibitor on the electrode surface. The protective nature of this film is reflected in the inhibition efficiency measurements obtained from chemical and electrochemical methods.

XRD study

The film formed on carbon steel surface exposed to 1.0 M HCl and 3.5% NaCl, in the absence and presence of inhibitor, was monitored using XRD to establish which elements constitute the layer on the carbon steel surface.

Analysis of the X-ray diffraction patterns of the film formed on carbon steel surface after immersion in both tested media (HCl & NaCl) showed that all the observed XRD peaks can be accounted for by the pattern reported for FeOOH. The characteristic peaks of FeOOH can be detected at $2\theta = 14.2, 27, 38, 47, 52, 68.4$ for both diffraction patterns but with different intensities as shown in Fig.10. It can be easily noticed that the peaks intensity in case of HCl media is much higher than that corresponding to the film formed in NaCl solution. This can be attributed to the fact that HCl solution is more aggressive media than NaCl.

Comparison of the observed XRD patterns of the film formed on carbon steel surface in presence of inhibitor with those in absence of inhibitor indicates that there is a marked difference between the constituents of the film in each case. As demonstrated in Fig.10, addition of TATSF to both tested media leads to corrosion control of carbon steel alloy as indicated from suppression of iron oxide signals. Also, the XRD patterns reveal the presence of amorphous organic layer on the alloy surface. From these previous observations it can be said that, the XRD results support the presence of adsorbed TATSF on carbon steel surface in both tested media.

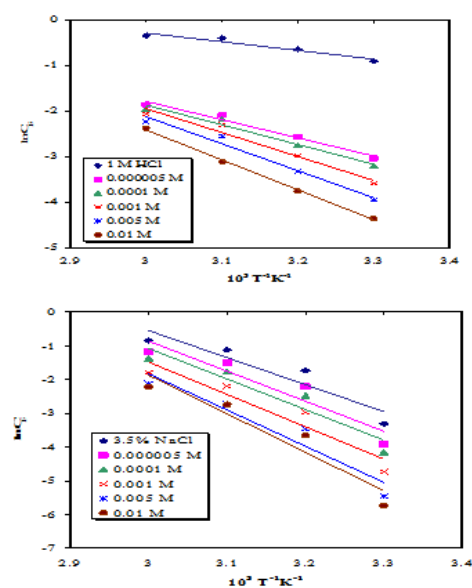


Fig.7. Arrhenius plots for carbon steel corrosion in 1 M HCl and 3.5% NaCl in the absence and presence of different concentrations of Schiff base compound.

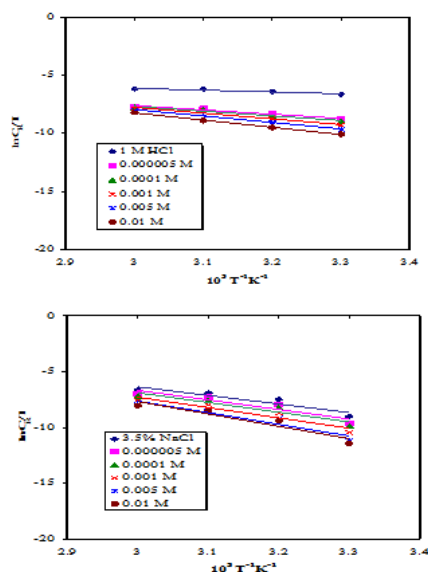


Fig. 8. Transition state plots for carbon steel corrosion in 1 M HCl and 3.5% NaCl in the absence and presence of different concentrations of Schiff base compound.

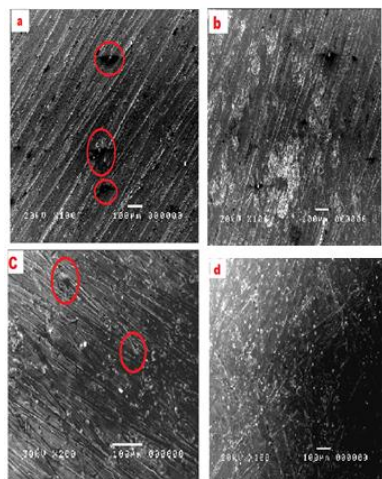


Fig. 9. SEM micrographs of CS after immersion for 48h in (a) HCl; (b) HCl+ inhibitor; (c) NaCl and (d) NaCl+inhibitor

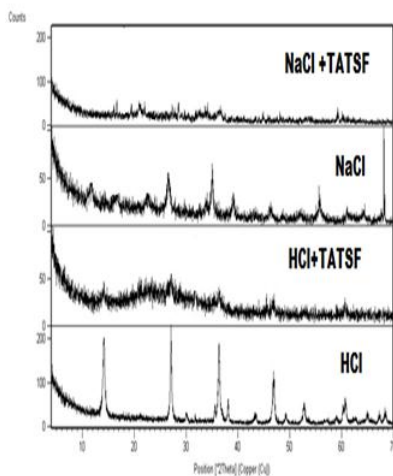


Fig.10. XRD patterns of the film formed on carbon steel surface after immersion in HCl and NaCl in absence and presence of inhibitor

IV CONCLUSION

According to the experimental results, the following important conclusions may be drawn from this work:

1. Novel Schiff base compound was synthesized and its chemical structure confirmed by elemental analysis, FT-IR and ¹H NMR spectroscopy.
2. The compound acts as efficient inhibitor for the corrosion of carbon steel in both studied media and the inhibition efficiency values increase with its concentration but decrease in temperature suggesting physical adsorption mechanism.
3. The adsorption mode was found to be obeyed Langmuir adsorption isotherm and the polarization curves indicate that the compound acts as mixed-type inhibitor in both studied media.
4. The ΔG_{ads}^0 values reveal that the interaction of the compound with metal surface may occur in both physical and chemical adsorption.
6. SEM and XRD studies confirmed the presence of a protective film on the metal surface in presence of the inhibitor.

ACKNOWLEDGMENT

The authors are greatly thankful to Egyptian Petroleum Research Institute (EPRI) for financial support.

REFERENCES

- [1] H.H. Uhlig, R.W. Revie, Corrosion and Corrosion Control, Wiley, New York, 1985.
- [2] V.S. Sastri, Corrosion Inhibitors, Principles and Application, John Wiley and Sons, 1998.
- [3] S. Hong, W. Chen, H.Q. Luo, N.B. Li, Inhibition effect of 4-aminoantipyrine on the corrosion of copper in 3 wt.% NaCl solution, Corros. Sci. 57 (2012) 270–278.
- [4] G. Banerjee, S.N. Malhotra, Contribution to adsorption of aromatic amines on mild steel surface from HCl solutions by impedance, UV, and Raman spectroscopy, Corrosion 48 (1992) 10–15.
- [5] A. Yurt, A. Balaban, S.U. Kandemir, G. Bereket, B. Erk, Investigation on some Schiff bases as HCl corrosion inhibitors for carbon steel, Mater. Chem. Phys. 85(2004) 420–426
- [6] I.B. Obot, E.E. Ebenso, M.M. Kabanda, Metronidazole as environmentally safe corrosion inhibitor for mild steel in 0.5 M HCl: experimental and theoretical investigation, J. Environ. Chem. Eng. 1 (2013) 431–439.
- [7] A.K. Singh, M.A. Quraishi, The effect of some bis-thiadiazole derivatives on the corrosion of mild steel in hydrochloric acid, Corros. Sci. 52 (2010) 1373–1385.
- [8] X. Li, S. Deng, H. Fu, G. Mu, Inhibition effect of 6-benzylaminopurine on the corrosion of cold rolled steel in H₂SO₄ solution, Corros. Sci. 51 (2009) 620–634.
- [9] S. Deng, X. Li, H. Fu, Alizarin violet 3B as a novel corrosion inhibitor for steel in HCl, H₂SO₄ solutions, Corros. Sci. 53 (2011) 3596–3602.
- [10] X.H. Li, S.D. Deng, H. Fu, Allyl thiourea as a corrosion inhibitor for cold rolled steel in H₃PO₄ solution, Corros. Sci. 55 (2012) 280–288.
- [11] S.D. Shetty, P. Shetty, H.V. Sudhaker Nayak, The inhibition action of N (furfuryl)-N'-phenyl thiourea on the corrosion of mild steel in hydrochloric acid medium, Mater. Lett. 61 (2007) 2347–2349.
- [12] Y. Tang, L. Yao, C. Kong, W. Yang, Y. Chen, Molecular dynamics simulations of dodecylamine adsorption on iron surfaces in aqueous solution, Corros. Sci. 53 (2011) 2046–2049.
- [13] H. Ju, Z.-P. Kai, Y. Li, Aminic nitrogen-bearing polydentate Schiff base compounds as corrosion inhibitors for iron in acidic media: a quantum chemical calculation, Corros. Sci. 50 (2008) 865–871.
- [14] M. Heydari, M. Javidi, Corrosion inhibition and adsorption behaviour of an amido-imidazoline derivative on API 5L X52 steel in

- CO₂-saturated solution and synergistic effect of iodide ions, *Corros. Sci.* 61 (2012) 148–155.
- [15] Emregül KC, Atakol O. Corrosion inhibition of mild steel with Schiff base compounds in 1 M HCl. *Mater Chem Phys* 2003;82:188–93.
- [16] M. B. Smith, J. March, *March's Advanced Organic Chemistry: Reactions, Mechanisms and Structure*, 6th ed., John Wiley & Sons, Inc., Hoboken, New Jersey, 2007.
- [17] F. A. Carey, *Organic Chemistry*, 5th ed., The McGraw-Hill Companies, Inc., New York, 2003.
- [18] U. Schiff, *Sopra dei nuova seria di basi organiche*, *Giornale di Scienze Naturali ed Economiche*, Vol. II, Palermo, 1–59 (1867).
- [19] T. T. Tidwell, Hugo (Ugo) Schiff, Schiff Bases, and a Century of β -Lactam Synthesis, *Angew. Chem. Int. Ed.*, 47, 1016–1020 (2008).
- [20] H. Ashassi-Sorkhabi, B. Shaabani, D. Seifzadeh, Corrosion inhibition of mild steel by some Schiff base compounds in hydrochloric acid, *Appl. Surf. Sci.* 239 (2005) 154–164.
- [21] Djamel Daoud; Tahar Douadi; Saifi Issaadi ; Salah Chafaa, Adsorption and corrosion inhibition of new synthesized thiophene Schiff base on mild steel X52 in HCl and H₂SO₄ solutions, *corrosion Science* 79 (2014) 50-58.
- [22] C.B. Pradeep Kumar, K.N. Mohana, Corrosion inhibition efficiency and adsorption characteristics of some Schiff bases at mild steel/hydrochloric acid interface, *Journal of the Taiwan Institute of Chemical Engineers* 45 (2014) 1031–1042.
- [23] Kaan C. Emregül, Raif Kurtaran, Orhan Atakol, An investigation of chloride-substituted Schiff bases as corrosion inhibitors for steel, *Corrosion Science* 45 (2003) 2803–2817.
- [24] D.K. Yadav, M.A. Quraishi, B. Maiti, Inhibition effect of some benzylidenes on mild steel in 1 M HCl: an experimental and theoretical correlation, *Corros. Sci.* 55 (2012) 254–266.
- [25] Mohamed A. Abbas, *Modification of Some Resin Materials Using Organometallic Compounds for Some Applications as Protection for Petroleum Equipments.. of science*, Al-Azhar University, 2011.
- [26] A. A. Farag, M.R. Noor El-Din, The adsorption and corrosion inhibition of some nonionic surfactants on API X65 steel surface in hydrochloric acid, *Corros. Sci.* 64 (2012) 174–183.
- [27] I. M. Nassar, Mohamed A. Abbas, A. hamdy and Olfat E. Elazabawy, Evaluating the inhibiting action of cds nanoparticles and CdS/PMMA hybrid for corrosion of carbon steel in acidic media, *international journal of current research*, vol. 5, issue, 12, pp.4327-4337, december, 2013.
- [28] Metal corrosion, erosion and wear, *Annual Book of ASTM Standards*, 03-02, G1-72, American Society for Testing and Materials, 1987.
- [29] N. Dkhireche, A. Dahami, A. Rochdi, J. Hmimou, R. Touir, M. Ebn Touhami, M. El Bakri, A. El Hallaoui, A. Anouar, H. Takenouti, Corrosion and scale inhibition of low carbon steel in cooling water system by 2-propargyl-5 hydroxyphenyltetrazole, *J. Ind. Eng. Chem.* 19 (2013) 1996–2003.
- [30] Elayyachy M., El Idrissi A., Hammouti B., New thiocompounds as corrosion inhibitor for steel in 1 M HCl. *Corros. Sci.* 48, 9, [2006], 2470–2479.
- [31] Lece H. D., Emregül K. C., Atakol O., Difference in the inhibitive effect of some Schiff base compounds containing oxygen, nitrogen and sulfur donors. *Corros. Sci.* 50, 5, 2008, 1460 - 1468.
- [32] S.S. Shivakumar, K.N. Mohana, Corrosion behavior and adsorptionthermodynamics of some schiff bases on mild steel corrosion in industrial water medium, *Int. J. Corros.* 13 (2013) 1–8.
- [33] Z. Tao, S. Zhang, W. Li, B. Hou, Corrosion inhibition of mild steel in acidic solution by oxo-triazole derivatives, *Corros. Sci.* 51 (2009) 2588–2595.
- [34] G. Bereket, A. Pinarbas_i, Electrochemical thermodynamic and kinetic studies of the behaviour of aluminium in hydrochloric acid containing various benzotriazole derivatives, *Corros. Eng. Sci. Technol.* 39 (2004) 308–312.
- [35] M.A. Hegazy, M.F. Zaky, Inhibition effect of novel nonionic surfactants on the corrosion of carbon steel in acidic medium, *Corros. Sci.* 52 (2010) 1333–1341.
- [36] Y.P. Khodyrev, E.S. Batyeva, E.K. Badeeva, E.V. Platova, L. Tiwari, O.G. Sinyashin, The inhibition action of ammonium salts of O,O'-dialkyldithiophosphoric acid on carbon dioxide corrosion of mild steel, *Corros. Sci.* 53 (2011) 976–983.
- [37] E.E. Oguzie, Y. Li, F.H. Wang, Corrosion inhibition and adsorption behavior of methionine on mild steel in sulfuric acid and synergistic effect of iodide ion, *J. Colloid Interface Sci.* 310 (2007) 90–98.
- [38] P.C. Okafor, Y.G. Zheng, Synergistic inhibition behaviour of methylbenzyl quaternary imidazoline derivative and iodide ions on mild steel in H₂SO₄ solutions, *Corros. Sci.* 51 (2009) 850–859.
- [39] I.B. Obot, N.O. Obi-Egbedi, Inhibition of aluminium corrosion in hydrochloric acid using nizoral and the effect of iodide ion addition, *Eur. J. Chem.* 7 (3) (2010) 837–843.
- [40] P.J. Flory, Inhibitive action of some plant extracts on the corrosion of steel in the acidic media, *J. Chem. phys.* 10 (1942) 51–61.
- [41] P.C. Okafor, C.B. Liu, X. Liu, Y.G. Zheng, F. Wang, C.Y. Liu, F. Wang, Corrosion inhibition and adsorption behavior of imidazoline salt on N80 carbon steel in CO₂-saturated solutions and its synergism with thiourea, *J. Solid State Electrochem.* 14 (2010) 1367–1376.
- [42] V.V. Torres, R.S. Amado, C.F. de Sa, T.L. Fernandez, C.A. Da Silva Riehl, A.G. Torres, E. D'Elia, Inhibitory action of aqueous coffee ground extracts on the corrosion of carbon steel in HCl solution, *Corros. Sci.* 53 (2011) 2385–2392.
- [43] H.Z. Alkhatlan, M. Khan, M.M.S. Abdullah, A.M. Al-Mayouf, A.A. Mousa, Z.A.M. Al-Othman, *Launaea nudicaulis* as a source of new and efficient green corrosion inhibitor for mild steel in acidic medium: A comparative study of two solvent extracts, *Int. J. Electrochem. Sci.* 9 (2014) 870–889.
- [44] Umoren SA, Obot IB, Ebenso EE, Okafor PC, Ogbobe O, Oguzie EE. Gum arabic as a potential corrosion inhibitor for aluminium in alkaline medium and its adsorption characteristics. *Anti-Corros Method Mater* 2006; 53:277–82.
- [45] H. Zarrok, A. Zarrouk, B. Hammouti, R. Salghi, C. Jama, F. Bentiss, Corrosion control of carbon steel in phosphoric acid by purpald – weight loss, electrochemical and XPS studies, *Corros. Sci.* 64 (2012) 243–252.
- [46] M.A. Hegazy , Ali M. Hasan, M.M. Emara, Mostafa F. Bakr, Ahmed H. Youssef, Evaluating four synthesized Schiff bases as corrosion inhibitors on the carbon steel in 1 M hydrochloric acid, *Corrosion Science* 65 (2012) 67–76.
- [47] T.P. Zhao, G.N. Mu, The adsorption and corrosion inhibition of anion surfactants on aluminium surface in hydrochloric acid, *Corros. Sci.* 41 (1999) 1937–1944.
- [48] T.P. Zhao, G.N. Mu, The adsorption and corrosion inhibition of anion surfactants on aluminium surface in hydrochloric acid *Corros. Sci.* 41 (1999) 1937-1944.
- [49] S.A. Soliman, M.S. Metwally, S.R. Selim, M.A. Bedair, Mohamed A. Abbas, Corrosion inhibition and adsorption behavior of new Schiff base surfactant on steel in acidic environment: Experimental and theoretical studies, *J. Ind. Eng. Chem.* 20 (2014) 4311–4320.
- [50] E.E. Ebenso, Inhibition of aluminium (AA3105) corrosion in HCl by acetamide and thiourea, *Corros. J.* 1 (1998) 29–44.
- [51] El-Tabei AS, Hegazy MA. A Corrosion Inhibition Study of a novel synthesized gemini nonionic surfactant for carbon steel in 1 M HCl Solution. *J Surfact Deterg* 2013. doi:10.1007/s11743-013-1457-1.
- [52] A.M. Fekry, Riham R. Mohamed, Acetyl thiourea chitosan as an eco-friendly inhibitor for mild steel in sulphuric acid medium, *Electrochim. Acta* 55 (2010) 1933–1939.
- [53] Weihua Li, Xia Zhao, Faqian Liu, Baorong Hou, Investigation on inhibition behavior of S-triazole–triazole derivatives in acidic solution, *Corros. Sci.* 50 (2008) 3261–3266.
- [54] Weihua Li, Xia Zhao, Faqian Liu, Baorong Hou, Investigation on inhibition behavior of S-triazole–triazole derivatives in acidic solution, *Corros. Sci.* 50 (2008) 3261–3266.
- [55] B. Doğru Mert, M.E. Mert, G. Kardas_, B. Yazıcı, Experimental and theoretical investigation of 3-amino-1,2,4-triazole-5-thiol as a corrosion inhibitor for carbon steel in HCl medium, *Corros. Sci.* 53 (2011) 4265–4272.
- [56] X.H. Li, S.D. Deng, G.N. Mu, H. Fu, F.Z. Yang, Inhibition effect of nonionic surfactant on the corrosion of cold rolled steel in hydrochloric acid, *Corros. Sci.* 50 (2008) 420–430.
- [57] I.N. Putilova, S.A. Balezin, V.P. Barannik, *Metallic Corrosion Inhibitors*, Pergamon Press, New York, 1960.
- [58] N.M. Guan, L. Xueming, L. Fei, Synergistic inhibition between o-phenanthroline and chloride ion on cold rolled steel corrosion in phosphoric acid. *Mater. Chem. Phys* 86 (2004) 59–68.

- [59] M. Bouklah, B. Hammouti, M. Lagrenee, F. Bentiss, Thermodynamic properties of 2,5-bis(4-methoxyphenyl)-1,3,4-oxadiazole as a corrosion inhibitor for mild steel in normal sulfuric acid medium. *Corros. Sci.* 48 (2006) 2831-2842.